

# Elastic plate impact onto water at high horizontal speed

Moritz Reinhard, Alexander Korobkin, Mark J. Cooker

School of Mathematics, University of East Anglia, Norwich NR4 7TJ, UK

E-mail: m.reinhard@uea.ac.uk

## 1 Introduction

We consider the free two-dimensional elastic plate impact onto water of infinite depth, initially at rest, with large constant horizontal velocity. The impact problem involves the coupling of the small angle of attack, the vertical motion, the plate bending and the water flow. Such a problem can be described as plate planing with an initially fast growth of the wetted region underneath the plate. The unsteady plate planing with small angle of attack has been well studied. Bessho [1] and Ulstein [2] analysed the influence of the water flow onto the oscillatory motion of a rigid plate. Makasyeyev [3] presented an approach of the elastic plate planing in heavy fluid by generalised functions. For plate impact with horizontal velocity a short-time planing analysis of the plate motion may be sufficient, especially when the plate rotation is determined as part of the solution. Recently Hicks & Smith [4] showed, in a shallow water approximation, that the plate exits the water a short time after the impact. We discuss the different scenarios of the plate motion depending on the initial configuration and we focus on the case when the plate gets fully wetted. It is shown, that the flexibility of the plate is the cause of large forces and leads to pressure distributions underneath the plate different from the pressure distributions of a rigid plate.

## 2 Mathematical formulation

The fluid is assumed to be inviscid and incompressible with constant density  $\rho_F$ . Initially, the fluid is at rest and occupies  $y' < 0$  of a Cartesian coordinate system  $x'Oy'$ . Initially, the plate, of length  $L$  and thickness  $h$ , has a small angle of attack  $\alpha \ll 1$  relative to the positive  $x'$ -axis and its left edge touches the free surface at  $O$ . The plate has initial vertical velocity component  $V$  in negative  $y'$ -direction and zero initial angular velocity. The horizontal velocity component  $U$  of the plate is constant along the positive  $x'$ -axis. The mass density  $\rho_S$  of the plate is constant. The elasticity of the plate is determined by its flexural rigidity  $D = Eh^3/(12(1 - \nu^2))$ , where  $E$  is Young's modulus and  $\nu$  is Poisson's ratio. We model the plate motion by Euler's beam equation supposing that  $h/L \ll 1$  and that the local slope of every point of the plate is of order  $\alpha$ . Due to the short time of impact we neglect gravity on the fluid, whereas gravity acts on the plate in the negative  $y$ -direction. The gravity acceleration is denoted by  $g$ . The nondimensional coordinates  $x$  and  $y$ , time  $t$ , fluid velocity potential  $\varphi(x, y, t)$  and pressure  $p(x, y, t)$  are scaled by  $L$ ,  $LU^{-1}$ ,  $\alpha UL$  and  $\alpha \rho U^2$ , respectively. A spatial coordinate, moving with the plate, is  $s(x) = x - t$ . The plate displacement  $y = \alpha \zeta(s, t)$  is given for  $0 < s < 1$ , i.e.  $t < x < t + 1$ . Under the forward part of the plate the free surface overturns and forms a thin low-pressure jet in  $x > t + c(t)$  (see Figure 1) which we neglect as it does not influence the plate motion. The plate interacts with the fluid from the trailing edge to the overturning point  $t < x < t + c$  only. The horizontal speed of the contact point  $1 + \dot{c}$  is assumed to be positive. The nondimensional

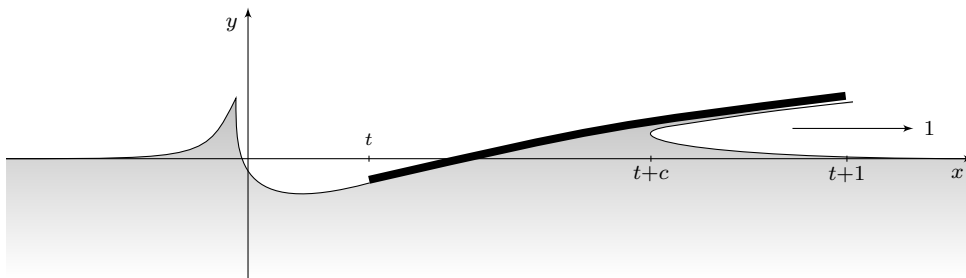


Figure 1: Plate impact onto deep water at time  $t$ . Nondimensional abscissae of trailing edge, contact point and front edge. The plate has nondimensional horizontal velocity 1.

initial vertical velocity  $\zeta_t(s, 0) = V\alpha^{-1}U^{-1}$  is assumed to be of order one. The free surface elevation is defined by  $y = \alpha\eta(x, t)$  in the wake region  $x < t$  and the upstream region  $x > t + c$ . The atmospheric pressure, here normalised to  $p = 0$ , acting on the free surface is constant. Surface tension, acoustic effects and the influence of air are neglected. Due to the small plate inclination and the small surface elevation, the boundary conditions can be linearised and projected onto  $y = 0$ . Basic relations are obtained by the mixed boundary value problem

$$\nabla^2\varphi(x, y, t) = 0 \quad (y < 0) \quad (1)$$

$$\varphi_y(x, 0, t) = \zeta_t(x - t, t) - \zeta_s(x - t, t) \quad (t < x < t + c) \quad (2)$$

$$\varphi(x, 0, t) = 0 \quad (x < 0, x > t + c) \quad (3)$$

$$\varphi(x, 0, t) = \tilde{\varphi}(x) \quad (0 < x < t) \quad (4)$$

$$\varphi(x, y, t) \rightarrow 0 \quad \text{as} \quad x^2 + y^2 \rightarrow \infty \quad (5)$$

where  $\tilde{\varphi}(x)$  in equation (4) is not  $t$ -dependent because  $\varphi_t = 0$  holds in the wake region. The following conditions of the two-dimensional high-speed planing outlined in Faltinsen [5] are used to determine the unknown functions  $\tilde{\varphi}(x)$  and  $c(t)$ : The contact point  $c$  is uniquely determined by Wagner's condition  $\eta(t + c, t) = \zeta(c, t)$  and  $\tilde{\varphi}(x)$  is obtained by Kutta's condition  $|\varphi_x(x, 0, t)| < \infty$  for  $x$  in a small vicinity of  $t$ . No shear forces or bending stresses act on the free ends of the plate, so we obtain free-free boundary conditions for the Euler beam equation:

$$\mu\zeta_{tt}(s, t) + \gamma\zeta_{ssss}(s, t) = p(s + t, 0, t) - \mu\kappa \quad (0 < s < 1) \quad (6)$$

$$\zeta_{ss}(0, t) = \zeta_{sss}(0, t) = 0 \quad \text{and} \quad \zeta_{ss}(1, t) = \zeta_{sss}(1, t) = 0. \quad (7)$$

The parameters are defined as  $\mu = \rho_S h \rho_F^{-1} L^{-1}$ ,  $\gamma = D \rho_F^{-1} L^{-3} U^{-2}$  and  $\kappa = g L \alpha^{-1} U^{-2}$ . We use Bernoulli's equation  $p = -\varphi_t$  to determine the pressure  $p$  acting on the plate. A solution of the plate deflection is sought in the expansion

$$\zeta(s, t) = \sum_{k=0}^{\infty} a_k(t) \psi_k(s) \quad (0 < s < 1) \quad (8)$$

in terms of the dry normal modes  $\psi_k(s)$  of the unforced equations (6) and (7). The modes  $\psi_0(s) = 1$  and  $\psi_1(s) = \sqrt{3}(2s - 1)$  are rigid-body modes of translation and rotation, and the other modes describe the plate bending.

### 3 Solution of the problem

The properties of the velocity potential described by the system (1)–(5) set the basis for all further calculations. Kutta's condition implies a singular Volterra integral equation of the first kind

$$\int_0^t \sqrt{\frac{t+c-\xi}{t-\xi}} \tilde{\varphi}_x(\xi) d\xi = \sum_{k=0}^{\infty} \frac{da_k}{dt} \int_0^c \sqrt{\frac{c-u}{u}} \psi_k(u) du - \sum_{k=0}^{\infty} a_k \int_0^c \sqrt{\frac{c-u}{u}} \psi_k'(u) du \quad (9)$$

w.r.t.  $\tilde{\varphi}_x$  (see Tuck [6]). The set of integral equations

$$\int_0^t \sqrt{\frac{t+c-\xi}{t-\xi}} \Phi_x(\xi, 0, t) d\xi = \sum_{k=0}^{\infty} a_k(t) \int_0^c \sqrt{\frac{c-u}{u}} \psi_k(u) du \quad (10)$$

$$\int_0^t \sqrt{\frac{t-\xi}{t+c-\xi}} \Phi_x(\xi, 0, t) d\xi = - \sum_{k=0}^{\infty} a_k(t) \int_0^c \sqrt{\frac{u}{c-u}} \psi_k(u) du \quad (11)$$

in terms of the displacement potential  $\Phi(x, y, t) = \int_0^t \varphi(x, y, \tau) d\tau$  are a consequence of Wagner's condition. Equation (10) confirms that the free water surface separates continuously from the trailing

edge. Equation (9) guarantees the smooth free surface separation and the continuity of the pressure function  $p(x, 0, t)$  at the trailing edge. In the wake region

$$\Phi_x(x, 0, t) = (t - x)\tilde{\varphi}_x(x) + \Phi_x(x, 0, x) \quad (0 < x < t) \quad (12)$$

can be formulated in terms of functions of a single variable. The kernels of the wake integrals in equations (9) and (10) have a square-root singularity at  $\xi = t$ . Thus, these equations are capable of evaluating  $\tilde{\varphi}_x(t)$  and  $\Phi_x(t, 0, t)$  by discretisation of the wake functions  $\tilde{\varphi}_x(x)$  and  $\Phi_x(x, 0, x)$  into piece-wise constant functions. An explicit pressure formula provides with (6) the second-order ODE system

$$M(c) \frac{d^2 a}{dt^2} = D(c, \dot{c}) \frac{da}{dt} + S(c, \dot{c}) a + b(c, \dot{c}) \int_0^t \sqrt{\frac{t - \xi}{t + c - \xi}} \tilde{\varphi}_x(\xi) d\xi - (\mu\kappa, 0, 0, \dots)^T \quad (13)$$

w.r.t.  $a(t) = (a_0(t), a_1(t), a_2(t), \dots)^T$  where the matrices  $D(c, \dot{c})$  and  $S(c, \dot{c})$ , the symmetric matrix  $M(c)$  and the vector  $b(c, \dot{c})$  are explicitly known. The time derivative of equation (11) completes the ODE system whose dependence on  $\tilde{\varphi}_x(x)$  and  $\Phi_x(x, 0, x)$  for  $x$  in a small vicinity of the trailing edge is negligible. The ODE system, calculating  $c(t)$  and  $a(t)$  with a modified Euler's method, and the integral equations (9) and (10) are alternately solved.

## 4 Numerical results

A sample of numerical results is presented for a steel plate impact onto water in Figure 2. The plate has length  $L = 2.4\text{m}$ , thickness  $h = 0.054\text{m}$ , plate density  $\rho_S = 7850\text{kg m}^{-3}$ , flexural rigidity  $D = 2860\text{kN m}$  and horizontal velocity  $U = 24\text{m s}^{-1}$ . We take the first seven normal modes for the elastic plate impact. To obtain the rigid plate behaviour only the two rigid modes are taken into account. The algorithm terminates (see Figure 2(a)) when either the plate exits the water ( $c = 0$ ) or the plate is fully wetted ( $c = 1$ ) or the instantaneous angle of attack  $\alpha a_1(t)$  is zero. The latter case happens when the trailing edge is lifting up and the plate rotates towards the water. This behaviour is critical because the plate front can touch the free surface before the plate is fully wetted so that an air bubble might be captured under the plate. Note that the distribution in Figure 2(a) would not change in the elastic plate case, but then for a few choices of  $\alpha$  and  $V$  the condition  $1 + \dot{c} > 0$  is not satisfied all the time. We focus on the case of  $\alpha = 8.6^\circ$  and  $V = 6\text{m s}^{-1}$ . The evolution of the elastic plate position and the position of its contact point  $x = t + c$  are shown in Figure 2(b). Due to the decreasing angle of attack the contact point moves rapidly forward especially at the end. The gravity force on the plate slightly influences the plate motion. For the rigid plate impact the behaviour of  $a_0(t)$ ,  $a_1(t)$  and  $c(t)$  does not differ significantly. In contrast, Figure 2(c) shows large differences in the force evolutions especially at the time  $t = 0.45$ , when the force peak magnitude of  $415\text{kN}$  is twice as large as it is for the rigid plate. After this peak, the force decreases faster and reaches almost zero afterwards. This can be explained by the bending of the plate towards the water surface and therefore faster contact point motion for time  $0.44 < t < 0.46$  than for the rigid plate. Finally, the front of the elastic plate bends back and entrains the water underneath the plate. The force evolution for the rigid plate can be interpreted as a time-averaged force of the elastic plate. Figure 2(d) shows the pressure distributions at the times when the force on the elastic plate reaches its peak ( $c(t = 0.45) \approx 0.88$  for rigid and elastic plate) and when the plate is fully wetted ( $c(t = 0.48) \approx 1$  for rigid and elastic plate). The pressure distribution of the rigid plate changes slowly, whereas the evolution of the pressure distribution of an elastic plate is more violent. The lower pressure values for the elastic plate in some regions makes it more likely that cavities could appear. The total energy decomposes into initial vertical kinetic energy and potential energy of the plate and the work done by the plate on the fluid to keep the horizontal velocity constant. The largest part of the total energy is dissipated as kinetic energy in the jet flux in front of the plate. A minor part is transferred into kinetic energy of the water flow (without jet energy). The energy contribution of the plate bending to the energy balance is negligible.

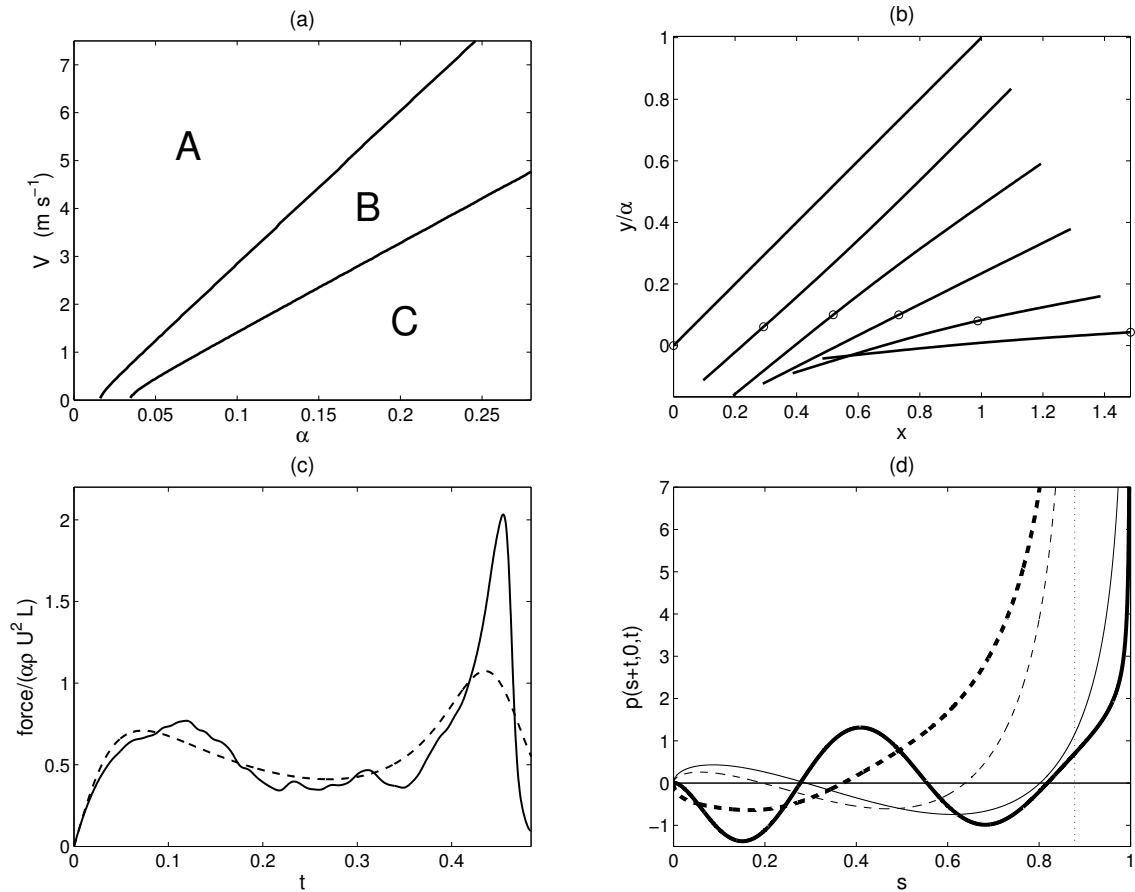


Figure 2: (a) Termination of the rigid plate impact due to  $c = 1$  (region A),  $a_1 = 0$  (region B) and  $c = 0$  (region C), (b) elastic plate and contact point position for  $t = 0, 0.10, 0.19, 0.29, 0.39, 0.48$ , (c) force evolution for the case of elastic plate (solid line) and rigid plate (dashed line), (d) pressure distribution for time  $t = 0.45$  (dashed lines) and  $t = 0.48$  (solid lines) for rigid (thin lines) and elastic plate impact (thick lines).

## 5 Summary

The results illustrate the ability to model and compute the interaction forces between a realistic elastic impacting free body with fixed forward speed and variable angle of attack and plate height and the fluid flow. In the presented example the analysis shows small differences in the motion of an elastic and rigid plate, but big differences occur in the force magnitude and pressure distribution acting on the plate. Pressure values smaller than the atmospheric pressure can already be found in the rigid plate impact, but an elastic plate reaches significantly lower pressure values. The work encourages further study of cavities and bubbles underneath an impacting plate as well as plate deformations due to forces larger than that predicted from a rigid-body analysis.

## References

- [1] M. Bessho & M. Komatsu. Two-dimensional unsteady planing surface. *Journal of Ship Research*, 28(1):18–28, 1984.
- [2] S. Ulstein & O.M. Faltinsen. Two-dimensional unsteady planing. *J. Ship Res*, 40(3):200–210, 1996.
- [3] M. Makasyeyev. Two dimensional unsteady planing of an elastic plate, June 2010. <http://www.icms.org.uk/downloads/hydro/Makasyeyev.ppt>.
- [4] P.D. Hicks & F.T. Smith. Skimming impacts and rebounds on shallow liquid layers. *Proceedings of the Royal Society of London A*, 2010. doi:10.1098/rspa.2010.0303.
- [5] O.M. Faltinsen. *Hydrodynamics of High-Speed Marine Vehicles*. Cambridge University Press, NY, 2005.
- [6] E.O. Tuck. A note on yawed slender wings. *Journal of Engineering Mathematics*, 13(1):47–62, 1979.